

Electronic Supplementary Information (ESI) for RSC Advances

## **Supplemental Information**

# **Organic Hydroperoxide Formation in the Acid-Catalyzed Heterogeneous Oxidation of Aliphatic Alcohols with Hydrogen Peroxide**

Qifan Liu, Weigang Wang\* , Ze Liu, Tianhe Wang, Lingyan Wu, Maofa Ge\*

Beijing National Laboratory for Molecular Sciences (BNLMS), State Key Laboratory for Structural Chemistry of Unstable and Stable Species, Institute of Chemistry, Chinese Academy of Sciences, Beijing, 100190, P. R. China

\*author to whom correspondence should be directed:

wangwg@iccas.ac.cn or gemaofa@iccas.ac.cn

## 1. Experimental Details

**Signal-photon Ionization Time of Flight Mass Spectrometer (SPI-TOFMS).** The variation of reactant gas concentration was monitored by SPI-TOFMS with a vacuum ultraviolet (VUV) laser ionization source. Reactant gas was ionized by 118 nm laser generated by focusing the third harmonic (355 nm, ~30 mJ per pulse) of a Nd:YAG laser in a tripling cell that contains about a 250 Torr argon/xenon (10/1) gas mixture. To separate the generated 118 nm laser beam from 355 nm fundamental beam, a magnesium fluoride prism (apex angle = 6°) is inserted to the laser beams. In this case, one is quite sure that the mass signal is by ionization purely through the VUV laser radiation with gentle power (~1 μJ per pulse, pulse duration ≈ 5 ns). The mass spectra of these three compounds obtained from the SPI-TOFMS are  $m/z = 44, 45, 59$  and  $74$  for 2-butanol,  $m/z = 59$  and  $73$  for 2-methyl-2-butanol and  $m/z = 43, 57$  and  $72$  for 3-buten-2-ol. The fragmentation ions produced by SPI-TOFMS are fewer than that ionized by electron ionization, but the main fragmentation ions have the similar mass number as shown in NIST Chemistry WebBook.<sup>1</sup> For each compound, most of the peaks were recorded during the measurements, and the strongest one was used to investigate the kinetics. Profiting from the multichannel on-line detection of the SPI-TOFMS, the new peaks produced by gas-phase products can be observed.

**Reactive Uptake Coefficients ( $\gamma$ ).** The heterogeneous kinetics can be quantified by the  $\gamma$ , which is defined as the probability that a gaseous molecule will be taken up irreversibly by the liquid. As an experiment just began, the movable injector was placed at its maximum position downstream. In this situation, the solution was

unexposed and the unperturbed concentration of reactant gas can be recorded as the original signal  $S_0$ . Then the injector was pulled upstream to expose the solution to the reactant gas. Reactive uptake was indicated by a constant offset between the original signal  $S_0$  and the reactive uptake signal with time,  $S$ . The observed first-order rate constant for removal of the reactant gas from gas-phase,  $k_{obs}$  ( $s^{-1}$ ) can be calculated from equation 1,

$$\ln\left(\frac{S}{S_0}\right) = -k_{obs} \frac{L}{v_{ave}} \quad (1)$$

where  $L$  (cm) is the contact distance of the reactant gas and the solution, and  $v_{ave}$  ( $cm\ s^{-1}$ ) is the average gas flow velocity of the reactant gas.  $k_{obs}$  can be determined more accurately by placing the injector at various positions in the reactor to change the contact distance. Figure S1a depicts the loss of 2-butanol signal as a function of injector position. The rate constant for removal of the reactant gas,  $k_{gas-liquid}$  ( $s^{-1}$ ), can be determined by correcting  $k_{obs}$  for diffusion:<sup>2-4</sup>

$$\frac{1}{k_{gas-liquid}} = \frac{1}{k_{obs}} + \frac{1}{k_{diff}} \left( k_{diff} = \frac{3.66D_i}{r^2} \right) \quad (2)$$

where  $r$  (cm) is the inner radius of the rotating cylinder,  $D_i$  ( $cm^2\ s^{-1}$ ) is the diffusion coefficient which can be calculated from the Hüller-Schettler-Giddings method,<sup>5</sup> and  $k_{diff}$  is the diffusion-limited rate ( $s^{-1}$ ). Fuller, Schettler and Giddings have developed a correlation equation based on special atomic diffusion volumes.<sup>5</sup> The equation is shown in equation 3,

$$D_{AB} = \frac{10^{-3} T^{1.75} (1/M_A + 1/M_B)^{1/2} \times 760}{p[(\sum_A v_i)^{1/3} + (\sum_B v_i)^{1/3}]^2} \quad (3)$$

where  $D_{AB}$  are the binary diffusion coefficients ( $\text{Torr cm}^2 \text{s}^{-1}$ ),  $T$  is the temperature (K),  $M_A$ ,  $M_B$  are the molecular weight ( $\text{g mol}^{-1}$ ),  $p$  is the pressure (Torr), and the  $v_i$  are the atomic diffusion volumes ( $\text{cm}^3$ ). The diffusion coefficients for aliphatic alcohols in the He-H<sub>2</sub>O vapor mixture can be estimated from the binary diffusion coefficients for aliphatic alcohols in helium and in water vapor:<sup>6</sup>

$$\frac{1}{D_i} = \left[ \left( \frac{y_2}{D_{12}} \right) + \left( \frac{y_3}{D_{13}} \right) \right] p_T \quad (4)$$

where  $D_i$  is the diffusion coefficients ( $\text{cm}^2 \text{s}^{-1}$ ) at  $p_T$ ,  $y_i$  is the mole fractions,  $D_{AB}$  is the binary diffusion coefficients ( $\text{Torr cm}^2 \text{s}^{-1}$ ), and  $p_T$  is the total pressure (Torr). It has been suggested that the correction of diffusion mentioned in this work would be applicable when the precondition,  $k_{obs} < k_{diff}/2$ , can be achieved.<sup>7</sup> All of our experimental data listed in Table S1 are fitted for this precondition. The percentage of  $k_{obs}$  to  $k_{gas-liquid}$  is calculated to evaluate the contribution of diffusion to  $k_{gas-liquid}$  in this study, the value of  $k_{obs}/k_{gas-liquid}$  is in the range of 0.5 to 1 in all experiments. Peclet number ( $P_e$ ) is also calculated to consider the influence of axial diffusion. The value of  $P_e$  (Table S1) is greater than ten for all experiments. In this situation, the flow velocity is much bigger than the axial diffusion and 3.66 can be used for the calculation of  $k_{diff}$ .<sup>2,4</sup> Finally, the  $\gamma$  can be acquired from equation 5,

$$\gamma = \frac{4k_{gas-liquid}V}{\omega A} \quad (5)$$

where  $\omega$  ( $\text{m s}^{-1}$ ) is the mean molecular speed of reactant gas,  $V$  ( $\text{cm}^3$ ) is the volume of the reaction zone, and  $A$  ( $\text{cm}^2$ ) is the geometric area of the exposed solution.

**GC-MS Analysis.** The chemical composition of the extracts was analyzed by Shimadzu GC-MS (model QP2010) according to the following parameters: column

HP-5 MS (internal diameter 0.25 mm, length 30 m, film thickness 0.25  $\mu\text{m}$ ), injection volume 1  $\mu\text{L}$ , inlet temperature 523K, detector temperature 473K. The column temperature was holding at 323K or 333K for 10 min. The reaction products were identified by comparing the mass spectra with those from NIST-2008 MS library software.

**ESI-MS Analysis.** The organic-phase extract was dissolved with a certain amount of methanol ( $\text{CH}_3\text{OH}$ ) before ESI-MS analysis. Given a certain loss of products in the water-phase and the dilution process before analysis, high concentration of  $\text{H}_2\text{O}_2$  (300mM) solutions were used during the aqueous-phase reactions to ensure the detection of products. The organosulfates formed by the aqueous-phase reactions were analyzed by Shimadzu ESI-MS (model LCMS-2010) according to following parameters: ESI nozzle voltage +1.6kV, injection volume 20  $\mu\text{L}$ , elution ( $\text{H}_2\text{O}:\text{CH}_3\text{OH}=50\%:50\%$ ) flow rate 0.1mL/min, capillary temperature 523K.

**Chemicals.** 2-butanol (99%, Alfa Aesar), 3-buten-2-ol (97%, Alfa Aesar), 2-methyl-2-butanol (98%, Alfa Aesar), *tert*-amyl hydroperoxide (85%, Lanzhou Auxiliary Agent Plant), di-*tert* amyl peroxide (95%, Lanzhou Auxiliary Agent Plant), *tert*-butyl alcohol (>99%, TCI), *tert*-butyl hydroperoxide (70%wt% aqueous solution, Alfa Aesar), di-*tert*-butyl peroxide(>94%, TCI), dichloromethane (99.9%, J&K),  $\text{H}_2\text{SO}_4$  (96 wt%, Beijing Chemical Reagents Co.),  $\text{H}_2\text{O}_2$  (35 wt% aqueous solution, Alfa Aesar) and  $\text{H}_2^{18}\text{O}_2$  (Sigma-Aldrich, 2% in  $\text{H}_2\text{O}$ , 90 atom %  $^{18}\text{O}$ ) were used as purchased. The reactant gas was prepared by injecting a compound into an evacuated 15 L glass flask to 3.8 Torr and pressurizing with helium to 1 atm. Reactant solution

were prepared by mixing deionized water (with resistivity of 18 MΩ cm) with H<sub>2</sub>SO<sub>4</sub> and H<sub>2</sub>O<sub>2</sub>. The H<sub>2</sub>SO<sub>4</sub> solution composition was checked before and after each experiment by titration with known NaOH solution and found to vary by less than 0.5wt%. The H<sub>2</sub>SO<sub>4</sub> solution was replaced after each uptake experiment.

## **2. Zaitsev's Rule**

According to the Zaitsev's rule, the alkene formed in greatest amount is the one that corresponds to removal of the hydrogen from the β-carbon having the fewest hydrogen substituents in elimination reactions. Thus, the formation of (E)-2-butene is reasonable because it has more substituents and tends to be more thermodynamically stable compared to other possible product such as 1-butene. Moreover, it has weaker steric hindrance compared to another possible product (Z)-2-butene.

**Table S1.** Summary of the experimental conditions, diffusion coefficients  $D_i$  used, calculated diffusion-limited rate  $k_{diff}$ , observed first-order rate constant  $k_{obs}$ , calculated Peclet number and reactive uptake coefficients ( $\gamma$ ).

Gas Reactant	H <sub>2</sub> SO <sub>4</sub> (wt %)	H <sub>2</sub> O <sub>2</sub> (wt %)	Flow Rate (STP cm <sup>3</sup> min <sup>-1</sup> )	$P_T$ (Torr)	$D_i$ (cm <sup>2</sup> s <sup>-1</sup> )	$k_{diff}$ (s <sup>-1</sup> )	$k_{obs}^*$ (s <sup>-1</sup> )	Peclet number	$\gamma^\dagger$ ( $\times 10^{-4}$ )	
2-butanol	60	0	220He	14.3	13.224	31.478	1.114	16.404	0.98±0.02	
	60	1	220He	14.6	12.631	30.066	0.938	16.821	0.82 ± 0.01	
	70	0	220He	14.4	12.967	30.866	2.167	16.613	1.98± 0.05	
	70	1	220He	14.1	13.416	31.935	2.338	16.398	2.01 ± 0.04	
2-methyl- 2-butanol	40	0	220He	24.0	/	/	/	/	/	
	40	1	220He	24.0	7.356	17.510	0.483	17.571	0.46 ± 0.02	
	50	0	220He	20.5	9.075	21.602	0.285	16.674	0.27± 0.02	
	50	0.1	220He	19.9	8.063	19.194	0.543	19.333	0.51±0.16	
	50	0.5	220He	20.4	7.832	18.470	2.120	19.415	2.21±0.15	
	50	1	220He	21.6	7.311	17.402	4.667	19.643	5.89±0.12	
	60	0	220He	21.4	8.318	19.799	1.939	17.426	1.99±0.04	
	60	0.1	220He	21.3	8.445	20.101	2.737	17.245	2.93±0.02	
	60	0.5	220He	21.8	7.972	19.047	4.614	17.849	5.65±0.15	
	60	1	220He	15.7	10.557	25.129	11.120	18.716	18.43 ±1.09	
	70	0	220He	21.0	9.138	21.752	8.347	16.165	12.52 ± 0.68	
	70	0.1	220He	16.5	12.341	29.377	10.894	15.234	16.00±0.03	
	70	0.5	220He	12.5	15.356	36.553	17.083	16.160	29.63±0.62	
	70	1	220He	5.9	35.039	83.405	38.628	15.005	66.49 ± 0.64	
	3-buten-2 -ol	50	0	220He	17.2	/	/	/	/	/
		50	1	220He	17.2	10.969	26.109	1.794	16.442	1.61±0.13
60		0	220He	15.5	12.978	30.089	1.258	15.421	1.10±0.07	
60		0.1	220He	16.4	13.731	32.685	1.460	13.775	1.28±0.04	
60		0.5	220He	16.6	13.721	32.660	1.780	13.619	1.57±0.04	
60		1	220He	15.5	12.978	30.893	7.023	15.421	7.60 ± 0.37	
70		0	220He	16.2	13.547	32.246	2.445	14.135	2.21±0.44	
70		0.1	220He	16.2	12.585	29.957	2.790	15.215	2.57±0.07	
70		0.5	220He	16.1	13.575	32.313	4.100	14.193	3.93±0.16	
70		1	220He	14.4	15.628	37.199	13.216	13.748	17.13 ± 0.32	

/ represents no obvious uptake.

\*The data is the average of at least three repetitious measurements.

†Each value is the average of at least three measurements, and the error corresponds to one standard deviation ( $\sigma$ ).

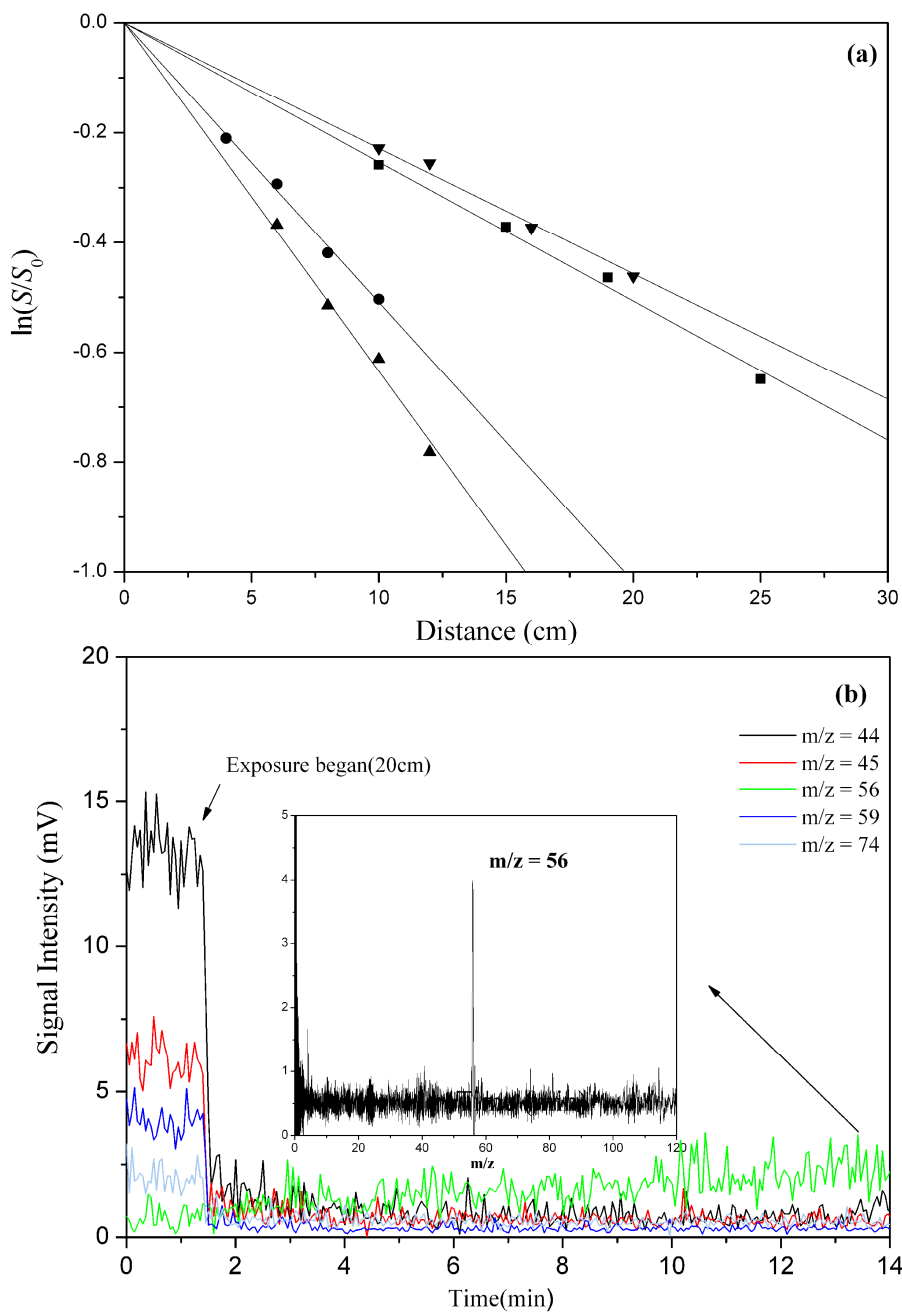


**Figure S1.** (a) 2-butanol signal loss as a function of exposed distance for 60wt% $H_2SO_4$ -1wt% $H_2O_2$ (▼), 60wt% $H_2SO_4$ (■), 70wt% $H_2SO_4$ (●) and 70wt% $H_2SO_4$ -1wt% $H_2O_2$ (▲) solution. (b) Real-time variation of all ion peaks during the uptake of 2-butanol into 70 wt%  $H_2SO_4$  solution. The insert plate is the real-time mass spectrum at the time marked by an long arrow.



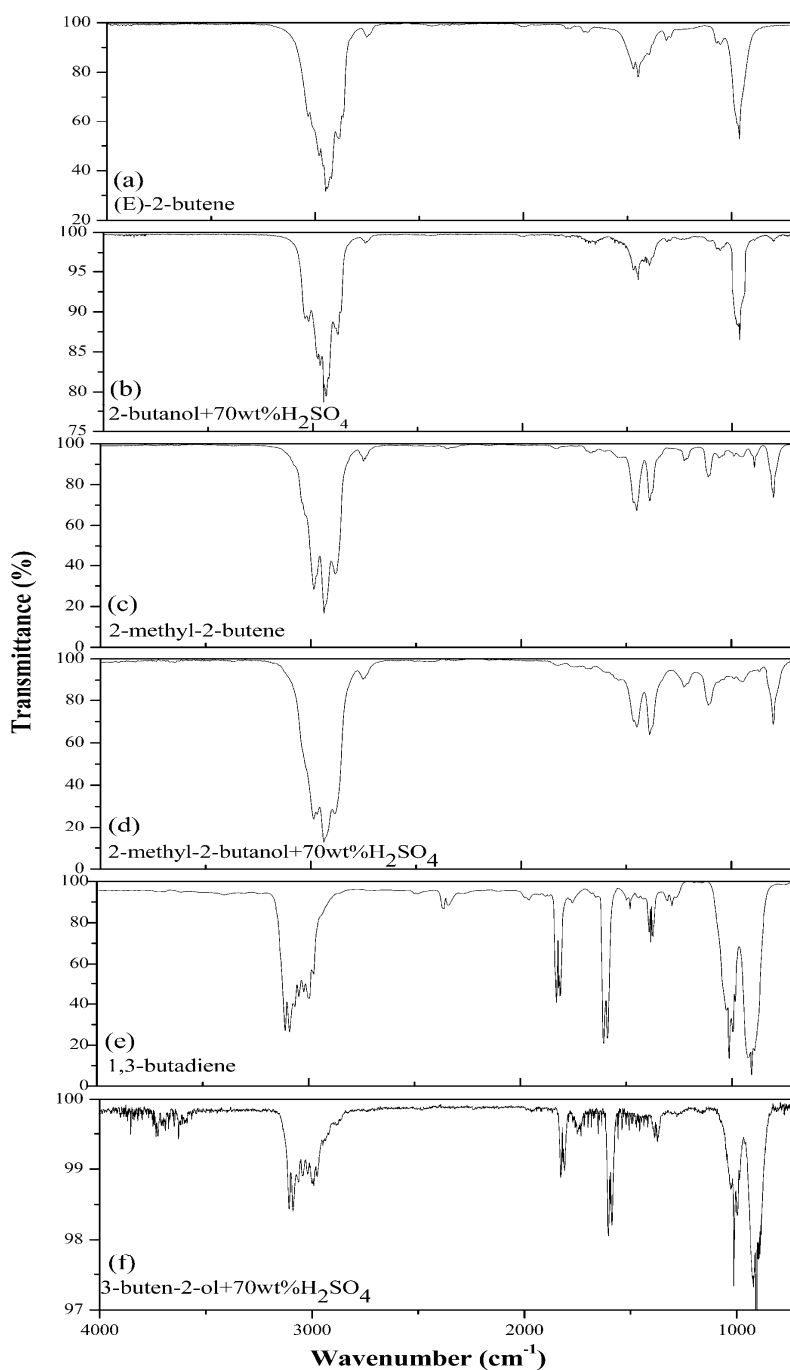


**Figure S2.** IR spectrum of (a) (E) -2-butene copied from NIST Chemistry WebBook; (b) gas-phase products formed during heterogeneous reaction of 2-butanol and 70wt% $\text{H}_2\text{SO}_4$  solution; (c) NIST 2-methyl-2-butene copied from NIST Chemistry WebBook; (d) gas-phase products formed during heterogeneous reaction of 2-methyl-2-butanol and 70wt% $\text{H}_2\text{SO}_4$  solution; (e) 1,3-butadiene copied from NIST Chemistry WebBook; (f) gas-phase products formed during heterogeneous reaction of 3-buten-2-ol and 70wt% $\text{H}_2\text{SO}_4$  solution. A series of weak peaks( $1300\text{cm}^{-1}$ - $1700\text{cm}^{-1}$  and  $3500\text{cm}^{-1}$ - $3900\text{cm}^{-1}$ ) in (f) are attributed to the water vapor interference.

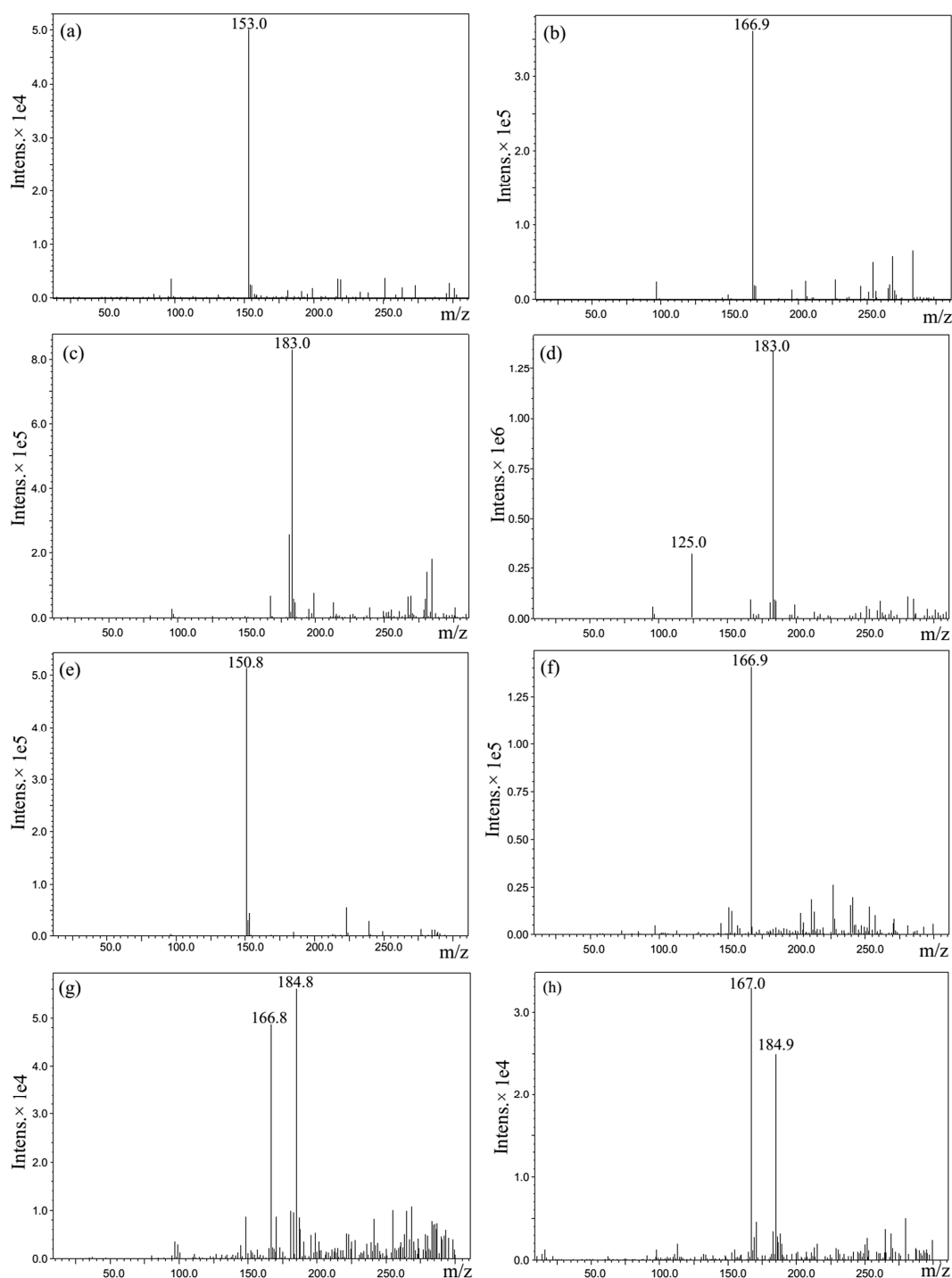


**Figure S3.** ESI-MS spectra (in the negative mode) of extracted organic-phase from aqueous-phase reactions between (a) 2-butanol and  $\text{H}_2\text{SO}_4$  (pH=1) solution; (b) 2-methyl-2-butanol and  $\text{H}_2\text{SO}_4$  (pH=1) solution; (c) 2-methyl-2-butanol and  $\text{H}_2\text{SO}_4$  (pH=1)- $\text{H}_2\text{O}_2$  (300mM) mixed solution; (d) TAHP and  $\text{H}_2\text{SO}_4$  (pH=1) solution; (e) 3-buten-2-ol and  $\text{H}_2\text{SO}_4$  (pH=1) solution; (f) 3-buten-2-ol and  $\text{H}_2\text{SO}_4$  (pH=1)- $\text{H}_2\text{O}_2$  (300mM) mixed solution; (g) *tert*-amyl sulfate and  $\text{H}_2^{18}\text{O}_2$  (2wt%) solution; (h) 2-methyl-2-butanol and  $\text{H}_2\text{SO}_4$  (pH=1)- $\text{H}_2^{18}\text{O}_2$  (1wt%) mixed solution.

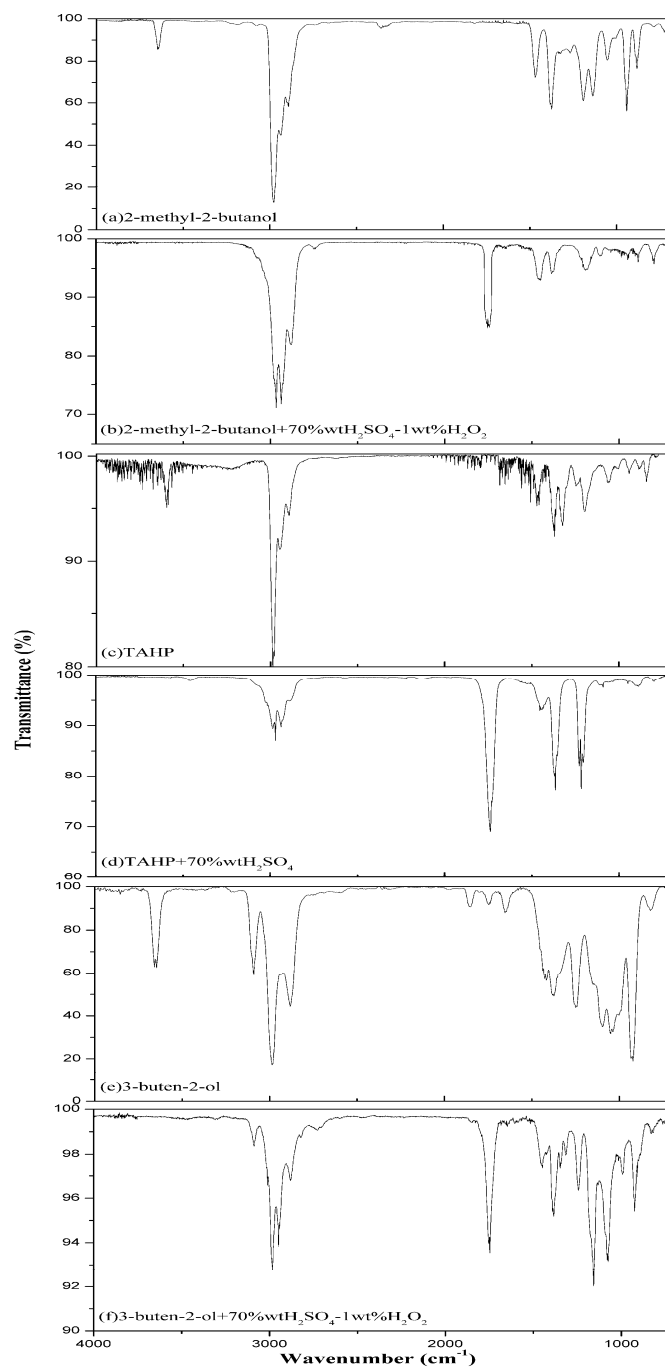


**Figure S4.** IR spectrum of (a) 2-methyl-2-butanol; (b) gas-phase products formed during heterogeneous reaction of 2-methyl-2-butanol and 70wt% $\text{H}_2\text{SO}_4$ -1wt% $\text{H}_2\text{O}_2$  mixed solution; (c)THAP; (d) gas-phase products formed during heterogeneous reaction of THAP and 70wt% $\text{H}_2\text{SO}_4$  solution; (e) 3-buten-2-ol; (f) gas-phase products formed during heterogeneous reaction of 3-buten-2-ol and 70wt% $\text{H}_2\text{SO}_4$ -1wt% $\text{H}_2\text{O}_2$  mixed solution.

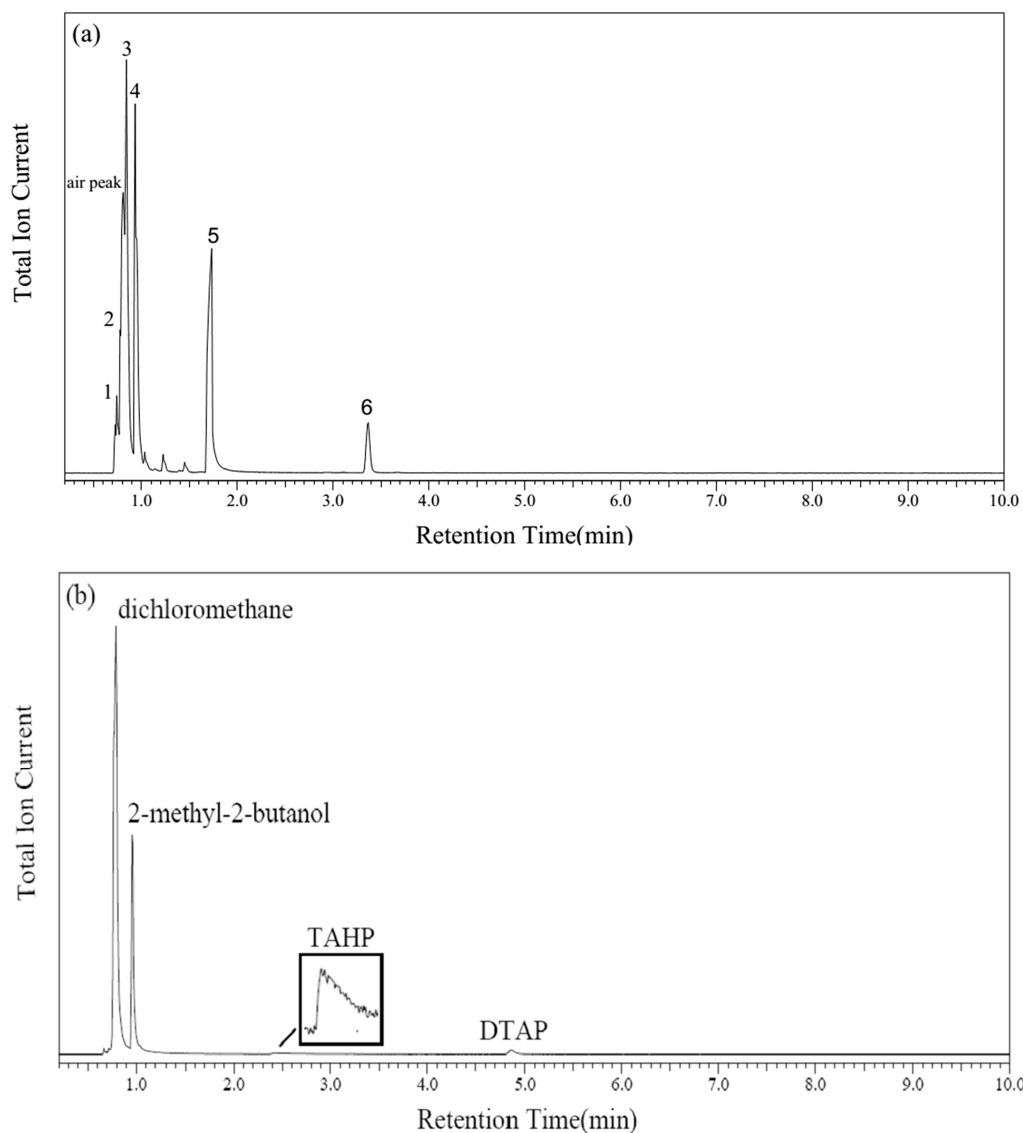


**Figure S5.** The gas chromatogram of the extracted organic-phase from aqueous-phase reactions between (a) 2-methyl-2-butanol and  $H_2SO_4$ (pH=1)- $H_2O_2$ (300mM) mixed solution; (b) 2-methyl-2-butanol and  $H_2SO_4$ (pH=1)- $H_2O_2$ (10mM) mixed solution. The column temperature were set at 333K and 323K for (a) and (b), respectively. The peaks 1-6 in (a) are attributed to butane, acetone, dichloromethane, 2-methyl-2-butanol, *tert*-amyl hydroperoxide (TAHP) and di-*tert*-amyl peroxide (DTAP), respectively.

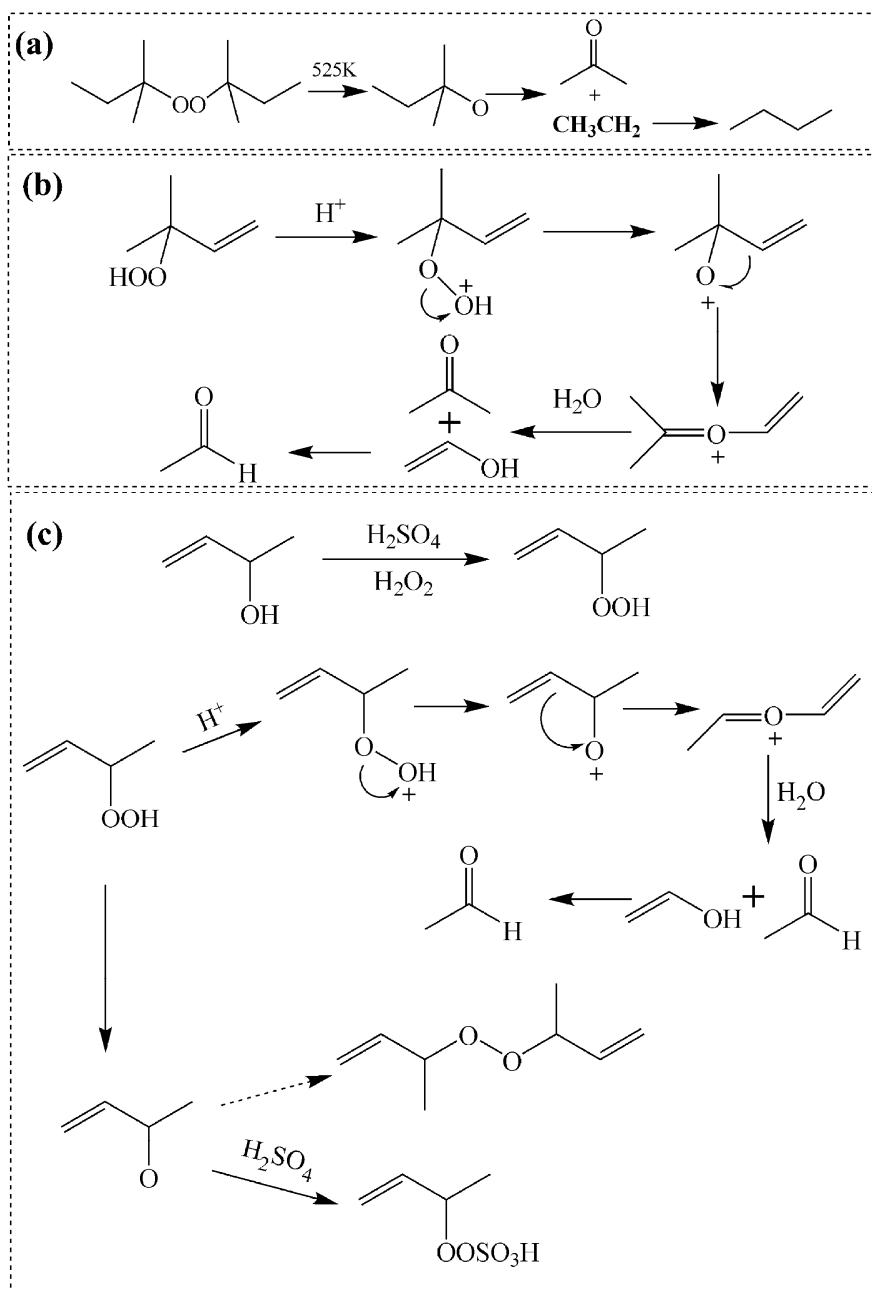


**Figure S6.** Proposed mechanism for (a) the pyrolysis of DTAP at 523K (adapted from reference 8); (b) the acid-catalyzed rearrangement of 1,1-dimethylallyl hydroperoxide (formed during the heterogeneous reaction of MBO and  $\text{H}_2\text{SO}_4$ - $\text{H}_2\text{O}_2$  mixed solution); (c) the degradation pathway of methylallyl hydroperoxide in  $\text{H}_2\text{SO}_4$  solution. The dashed arrow in (c) means a possible route for the formation of methylallyl hydrogen peroxysulfate.

## References

- (1) NIST Chemistry WebBook. <http://webbook.nist.gov/chemistry/>
- (2) Murphy, D. M.; Fahey, D. W. Mathematical treatment of the wall loss of a trace species in denuder and catalytic-converter tubes. *Anal. Chem.* 1987, 59, (23), 2753-2759.
- (3) Hanson, D. R.; Burkholder, J. B.; Howard, C. J.; Ravishankara, A. R. Measurements of OH and HO<sub>2</sub> radical uptake coefficients on water and sulfuric-acid surfaces. *J. Phys. Chem.* 1992, 96, (12), 4979-4985.
- (4) Gershenzon, Y. M.; Grigorieva, V. M.; Ivanov, A. V.; Remorov, R. G. O<sub>3</sub> and OH sensitivity to heterogeneous sinks of HO<sub>x</sub> and CH<sub>3</sub>O<sub>2</sub> on aerosol particles. *Faraday Discuss.* 1995, 100, 83-100.
- (5) Fuller, E. N.; Schettler, P. D.; Giddings, J. C. A new method for prediction of binary gas-phase diffusion coefficients. *Ind. Eng. Chem. Res.* 1966, 58, 19-27.
- (6) Fairbanks, D. F.; Wilke, C. R. Diffusion coefficients in multicomponent gas mixtures. *Ind. Eng. Chem. Res.* 1950, 42, 471-475.
- (7) Noziere, B.; Voisin, D.; Longfellow, C. A.; Friedli, H.; Henry, B. E.; Hanson, D. R. The uptake of methyl vinyl ketone, methacrolein, and 2-methyl-3-butene-2-ol onto sulfuric acid solutions. *J. Phys. Chem. A* 2006, 110, (7), 2387-2395.
- (8) Milas, N. A.; Surgenor, D. M. Studies in organic peroxides. X. Tert-amyl hydroperoxide and di-tert-amyl peroxide. *J. Am. Chem. Soc.* 1946, 68, (4), 643-644.